

# The Generalized Microscopic Image Reconstruction Problem

**Amotz Bar-Noy**

City University of New York (CUNY), USA  
amotz@sci.brooklyn.cuny.edu

**Toni Böhnlein**

Bar Ilan University, Ramat-Gan, Israel  
toni.bohnlein@biu.ac.il

**Zvi Lotker**

Ben Gurion University of the Negev, Beer Sheva, Israel  
Bar Ilan University, Ramat-Gan, Israel  
zvi.lotker@gmail.com

**David Peleg**

Weizmann Institute of Science, Rehovot, Israel  
david.peleg@weizmann.ac.il

**Dror Rawitz**

Bar Ilan University, Ramat-Gan, Israel  
dror.rawitz@biu.ac.il

---

## Abstract

This paper presents and studies a generalization of the *microscopic image reconstruction* problem (*MIR*) introduced by Frosini and Nivat [7, 12]. Consider a specimen for inspection, represented as a collection of points typically organized on a grid in the plane. Assume each point  $x$  has an associated physical value  $\ell_x$ , which we would like to determine. However, it might be that obtaining these values precisely (by a *surgical probe*) is difficult, risky, or impossible. The alternative is to employ *aggregate* measuring techniques (such as EM, CT, US or MRI), whereby each measurement is taken over a larger window, and the exact values at each point are subsequently extracted by computational methods.

In this paper we extend the MIR framework in a number of ways. First, we consider a generalized setting where the inspected object is represented by an arbitrary graph  $G$ , and the vector  $\ell \in \mathbb{R}^n$  assigns a value  $\ell_v$  to each node  $v$ . A probe centered at a vertex  $v$  will capture a window encompassing its entire neighborhood  $N[v]$ , i.e., the outcome of a probe centered at  $v$  is  $\mathcal{P}_v = \sum_{w \in N[v]} \ell_w$ . We give a criterion for the graphs for which the extended MIR problem can be solved by extracting the vector  $\ell$  from the collection of probes,  $\bar{\mathcal{P}} = \{\mathcal{P}_v \mid v \in V\}$ .

We then consider cases where such reconstruction is impossible (namely, graphs  $G$  for which the probe vector  $\mathcal{P}$  is inconclusive, in the sense that there may be more than one vector  $\ell$  yielding  $\mathcal{P}$ ). Let us assume that surgical probes (whose outcome at vertex  $v$  is the exact value of  $\ell_v$ ) are technically available to us (yet are expensive or risky, and must be used sparingly). We show that in such cases, it may still be possible to achieve reconstruction based on a *combination* of a collection of standard probes together with a suitable set of surgical probes. We aim at identifying the minimum number of surgical probes necessary for a unique reconstruction, depending on the graph topology. This is referred to as the MINIMUM SURGICAL PROBING problem (MSP).

Besides providing a solution for the above problems for arbitrary graphs, we also explore the range of possible behaviors of the MINIMUM SURGICAL PROBING problem by determining the number of surgical probes necessary in certain specific graph families, such as perfect  $k$ -ary trees, paths, cycles, grids, tori and tubes.

**2012 ACM Subject Classification** Mathematics of computing

**Keywords and phrases** Discrete mathematics, Combinatorics, Reconstruction algorithm, Image reconstruction, Graph spectra, Grid graphs



© Amotz Bar-Noy, Toni Böhnlein, Zvi Lotker, David Peleg, and Dror Rawitz;  
licensed under Creative Commons License CC-BY

30th International Symposium on Algorithms and Computation (ISAAC 2019).

Editors: Pinyan Lu and Guochuan Zhang; Article No. 42; pp. 42:1–42:15

Leibniz International Proceedings in Informatics



LIPIC Schloss Dagstuhl – Leibniz-Zentrum für Informatik, Dagstuhl Publishing, Germany

Digital Object Identifier 10.4230/LIPIcs.ISAAC.2019.42

Funding This work was supported by US-Israel BSF grant 2018043.

Amotz Bar-Noy: ARL Cooperative Grant, ARL Network Science CTA, W911NF-09-2-0053

Dror Rawitz: ISF grant no. 497/14

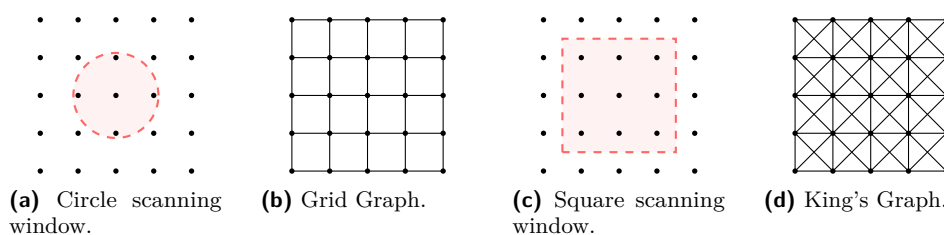
## 1 Introduction

**Background and motivation.** Imaging technologies are used increasingly widely in a variety of medical, engineering, and scientific application domains. Imagine a specimen for inspection, represented as a collection of points organized in (2- or 3-dimensional) space. Assume each point  $x$  has an associated physical value  $\ell_x$  (e.g., atom density, brightness, etc). Our goal is to determine these values at all points in the specimen. However, it is often the case that obtaining these values through a direct and precise inspection (hereafter referred to as a *surgical probe*) is complicated, prohibitively expensive, potentially risky, or even impossible. A commonly used alternative is to employ *aggregate* measuring techniques (such as EM, CT, US or MRI), whereby measurements are taken over a larger area (rather than a single point), and the (exact or approximate) values at each point are subsequently extracted by computational methods. For example, a microscope with a scanning window can be used for inspecting the specimen by systematically going over it and *probing* (i.e., taking a measurement in) each window. The measurement taken from each window centered at point  $x$ , hereafter denoted by  $\mathcal{P}_x$ , consists of the sum of the observed values at all the points in the observed window. (This is sometimes referred to as the *luminosity* of the window.) The goal is then to use the measurements obtained by a sufficiently diverse collection of probes in order to deduce the original values  $\ell_x$  at each point  $x$  in the specimen.

This general problem has been extensively studied as the *discrete tomography* reconstruction problem (*DTR*). For a survey, see Herman and Kuba [10]. The *microscopic image reconstruction* problem (*MIR*) was then introduced by Frosini and Nivat in [7, 12] as a natural extension of the DTR problem. In both problems, the specimen is represented by a 2-dimensional grid (see Figure 1b) whose points,  $x = (i, j)$ , for  $i \in \{1, \dots, n_1\}$  and  $j \in \{1, \dots, n_2\}$ , are assigned nonnegative integer<sup>1</sup> values  $\ell_{i,j}$ . In the DTR problem, the window of a probe is typically an entire row or column (i.e., the probe can be thought of as performed by a ray piercing the specimen from one side to the other). In the MIR problem, it is assumed that the microscope's scanning window is a segment of the plane (e.g., a circle or a rectangle). For example, assume for the sake of illustration that the window corresponds to a circle of radius 1 (see Figure 1a). Then the input can be thought of as an  $n_1 \times n_2$  integer matrix, and the output is an  $n_1 \times n_2$  integer matrix. A similar setting can be described with a square scanning window as shown in Figure 1c. A window consisting of a node and its eight neighbors in the grid is depicted by the king's graph, illustrated in Figure 1d.

In this paper we extend the MIR framework of [7] in a number of ways. First, we consider a generalized setting where the inspected object is represented by an arbitrary simple undirected connected graph  $G = (V, E)$  with vertex set  $V = \{1, \dots, n\}$ . Given a graph  $G$ , the vector  $\ell \in \mathbb{R}^n$  is an assignment of a value  $\ell_v$  to each node  $v$ . Given a graph  $G$  and a vector  $\ell \in \mathbb{R}^n$ , define  $\ell(U) \triangleq \sum_{v \in U} \ell_v$ , for every  $U \subseteq V$ . Here, a probe centered at a vertex  $v$  captures a window encompassing its entire neighborhood,  $N[v] \triangleq \{w \mid (v, w) \in E\} \cup \{v\}$ , i.e., the outcome of a probe centered at  $v$  is  $\mathcal{P}_v \triangleq \ell(N[v]) = \sum_{w \in N[v]} \ell_w$ . For example, in

<sup>1</sup> In fact, [7] assume only Boolean values, 0 or 1.



■ **Figure 1** Scanning windows for the grid.

the case of a grid specimen,  $N[v]$  may contain all vertices at distance at most  $d$  (according to any norm  $L_p$ ) from  $v$ . Our first question is to determine the class of graphs for which the extended MIR problem can be solved, namely, for which it is possible to extract the vector  $\ell$  from the collection of probes at all vertices,  $\bar{\mathcal{P}} = \{\mathcal{P}_v \mid v \in V\}$ .

Note, however, that in some cases, this type of reconstruction is not possible. Given a graph  $G$  and a probe vector  $\mathcal{P}$ , it may be possible that the outcome of the measurements is inconclusive, in the sense that there may be several (or even infinitely many) vectors  $\ell$  that would yield the same probe vector  $\mathcal{P}$ . For example, consider the case where  $G$  consists of two nodes and an edge between them. In this case, the same probe vector  $\mathcal{P} = (p_1, p_2)$  is obtained for any vector  $(\ell_1, \ell_2)$  such that  $\ell_1 + \ell_2 = p_1 = p_2$ .

This leads to our next extension of the problem. Let us assume that surgical probes (whose outcome at vertex  $v$  is the exact value of  $\ell_v$ ) are technically available to us, yet are so expensive or risky that we must use them sparingly. In cases where a unique reconstruction based on standard (aggregate) probes alone is not possible, it may still be possible to achieve a reliable reconstruction based on a combination of a comprehensive collection of standard probes together with a (hopefully small) set of surgical probes. Hence, our second goal is to identify the minimum number of surgical probes necessary for a unique reconstruction, depending on the graph topology. Formally, we consider the following MINIMUM SURGICAL PROBING problem (MSP). Given a graph  $G$  and a vector  $\mathcal{P}$ , the goal is to find the actual vector  $\ell$  that generated  $\mathcal{P}$ , using as few surgical probes as possible.

**Our results.** In Section 2 we present an efficient algorithm for solving the MINIMUM SURGICAL PROBING problem. We show that one can compute the minimum number of surgical probes necessary for any graph and determine a subset of the vertices which need to be probed. The general problem can be formulated as a system of linear equations. The adjacency matrix of our graph (whose main diagonal is set to 1) determines the coefficient matrix and the probe vector  $\mathcal{P}$  is the right hand side. We use techniques from linear algebra to solve the problem.

While these results allow us to determine the number of surgical probes necessary for every graph, it is interesting to explore and chart the range of possible behaviors of the problem, by identifying the number of surgical probes necessary for some specific graph families. Towards this goal, we consider (in Section 3) the behavior of the problem on trees. We first show that  $\ell$  can be uncovered on any  $n$ -vertex tree using  $\lfloor \frac{n}{2} \rfloor - 1$  many surgical probes, and that this number is tight if  $n$  is odd. In contrast we show that on the class of perfect  $k$ -ary trees, no surgical probes are required to uncover  $\ell$ .

We continue pursuing this line of investigation by considering (in Section 4) *Cartesian products* of paths and cycles, resulting in *grids*, *tubes* and *tori*. Furthermore, Section 5 deals with the *Strong product* of two path graphs, which is known as the king's graph (see Figure 1d). Grid graphs are interesting as they have the topology which was studied in previous papers on discrete tomography. A probe  $\mathcal{P}$  has a circular scanning window. Similarly, in the king's graph a probe  $\mathcal{P}$  has a square scanning window.

## 42:4 The Generalized Microscopic Image Reconstruction Problem

As we will see, the number of required surgical probes is related to the rank of our graph's adjacency matrix which in turn is related to its eigenvalues. The eigenvalues of adjacency matrices are studied in spectral graph theory. Simple expressions to determine the eigenvalues for adjacency matrices of path and cycle graphs are known. This and the fact that Cartesian and Strong products preserve the eigenvalues of their factor's adjacency matrices allow us to derive expressions for the eigenvalues of the grids, tubes, tori and king's graph adjacency matrices. We use these expressions to determine the number of surgical probes in a more efficient way than our general result allows for.

Table 1 lists the number of surgical probes that are sufficient to discover  $\ell$  for grids, tubes, tori and king's graphs. To express our results, we introduce the following indicator variables:

$$\mathcal{I}_b^a(n) \triangleq \begin{cases} 1 & \text{if } n \bmod a \equiv b \\ 0 & \text{otherwise.} \end{cases}$$

Surprisingly, only a constant number of surgical probes are needed for any grid, tube, or torus. On the other hand, the king's graph may require as many as  $n_1 + n_2 - 1$  probes. In addition, in all the above graphs the number of probes may be zero, depending on the graph dimensions. For example, when both  $n_1$  and  $n_2$  are multiples of 30, a grid of size  $n_1 \times n_2$  does not require surgical probes. Similarly, when  $n_1$  and  $n_2$  are multiples of 3, no surgical probes are required for the king's graph. Hence, when given control on the dimensions (say, in a design phase), one may fix the dimensions such that no surgical probes are required.

Note that, these results give us only the number of surgical probes that are sufficient to uncover  $\ell$ . In general, we need to resort to our result from Section 2 to find a set of vertices that needs to be probed. For paths and cycles, however, it is possible to find these vertices directly and uncover  $\ell$  in linear time.

■ **Table 1** The table shows the number of surgical probes. In the case of a tube  $n_1$  is the length of the path while  $n_2 \geq 3$  is the length of the cycle.

Graph	# surgical probes	at most
Grid	$\mathcal{I}_2^3(n_1)\mathcal{I}_1^2(n_2) + \mathcal{I}_1^2(n_1)\mathcal{I}_2^3(n_2) + 2\mathcal{I}_4^5(n_1)\mathcal{I}_4^5(n_2)$	4
Path ( $n_2 = 1$ )	$\mathcal{I}_2^3(n_1)$	1
Tube	$2\mathcal{I}_1^2(n_1)\mathcal{I}_0^3(n_2) + \mathcal{I}_2^3(n_1)\mathcal{I}_0^2(n_2) + 2\mathcal{I}_2^3(n_1)\mathcal{I}_0^4(n_2) + 4\mathcal{I}_4^5(n_1)\mathcal{I}_0^5(n_2)$	9
Cycle ( $n_1 = 1$ )	$2\mathcal{I}_0^3(n_2)$	2
Torus	$4\mathcal{I}_0^3(n_1)\mathcal{I}_0^4(n_2) + 4\mathcal{I}_0^4(n_1)\mathcal{I}_0^3(n_2) + 2\mathcal{I}_0^2(n_1)\mathcal{I}_0^6(n_2) + 2\mathcal{I}_0^6(n_1)\mathcal{I}_0^2(n_2) + 8\mathcal{I}_0^5(n_1)\mathcal{I}_0^5(n_2)$	20
King's graph	$\mathcal{I}_2^3(n_1)n_2 + \mathcal{I}_2^3(n_2)n_1 - \mathcal{I}_2^3(n_1)\mathcal{I}_2^3(n_2)$	$n_1 + n_2 - 1$

**Related Work.** Most important for our work is the extension of the DTR problem by Frosini and Nivat [7, 12]. They introduced the problem of reconstructing a binary matrix from a rectangular scan instead of the row and column sums. A polynomial time algorithm is presented that solves the reconstruction problem for a class of matrices. Battaglino, Frosini and Rinaldi [4] extended this by studying scans of different shapes like diamond shapes. Relations to tiling are discovered.

A concept similar to surgical probing was considered by Frosini, Nivat and Rinaldi [8]. They analyze a variation where a grid is scanned by the means of two rectangular windows. To solve the reconstruction problem, they assume that a small number of the values associated with the grid points are known in advance.

A combination of DTR and MIR is studied by Alpers and Gritzmann [1]. Their goal is to reconstruct a matrix from column and row sums with additional windows constraints. In [3] they study applications to image reconstruction.

Gritzmann et al. [9] show that determining the minimum number of prescribed values making the DTR problem unique is in general a NP-hard problem. Prescribed values are an analogue to surgical probes. The hardness results from the integer values in the DTR problem. Alpers and Gritzmann [2] discuss uniqueness problems for a dynamic variation of DTR. Here, the application is to track particles over time.

## 2 Algorithm for Solving Minimum Surgical Probing

In this section, we show how to solve the MINIMUM SURGICAL PROBING problem. We start with some preliminaries. Denote the  $n \times n$  identity matrix by  $I_n$ . Given a matrix  $A$ , let  $\text{rank}(A)$  denote its rank, and let  $\Lambda(A)$  denote its set of eigenvalues. For an eigenvalue  $\lambda \in \Lambda(A)$ , denote by  $\phi(\lambda, A)$  the multiplicity of  $\lambda$  in  $\Lambda(A)$ .

Given a graph  $G$ , let  $A_G = \{a_{ij}\}$  be  $G$ 's  $n \times n$  adjacency matrix, i.e.,

$$a_{ij} = \begin{cases} 1, & (i, j) \in E, \\ 0, & \text{otherwise.} \end{cases}$$

Define  $\bar{A}_G \triangleq A_G + I_{|V|}$  as the adjacency matrix whose main diagonal is set to 1.

A probe vector  $\mathcal{P}$  is induced by  $\ell \in \mathbb{R}^n$  if the following is satisfied:

$$\bar{A}_G \cdot \ell = \mathcal{P}. \tag{1}$$

► **Lemma 1.** *The multiplicity of the eigenvalue -1 in the matrix  $A_G$  is*

$$\phi(-1, A_G) = \phi(0, \bar{A}_G) = |V| - \text{rank}(\bar{A}_G).$$

**Proof.** If  $\bar{A}_G$  has an eigenvalue 0, then it is singular. Indeed, the multiplicity of the eigenvalue 0 is the dimension on the kernel (null-space)  $\ker(\bar{A}_G)$  (cf. [5]). The eigenspace of an eigenvalue  $\lambda$  consists of the solutions to  $(\bar{A}_G - \lambda I_{|V|})x = 0$ . Therefore, the eigenspace of eigenvalue 0 is the kernel of  $\bar{A}_G$ . If 0 is an eigenvalue of  $\bar{A}_G$ , then  $-1$  is an eigenvalue of  $A_G$ , and the multiplicity is the same. ◀

We now present our general result.

► **Theorem 2.** *Consider a graph  $G$  and a probe vector  $\mathcal{P}$ .*

1. *If the adjacency matrix  $\bar{A}_G$  has full rank, i.e.,  $\text{rank}(\bar{A}_G) = |V|$ , then  $\ell$  can be uncovered in polynomial time without using any surgical probes.*
2. *Otherwise, the minimum number of surgical probes needed to uncover  $\ell$  is  $s = \phi(-1, A_G)$ . Moreover, a set of  $s$  nodes whose surgical probes uncover  $\ell$  can be computed in polynomial time.*

**Proof.** As mentioned above, the label vector  $\ell \in \mathbb{R}^{|V|}$  satisfies the system of linear equations given in (1). Therefore, system (1) has at least one solution. If the adjacency matrix  $\bar{A}_G$  has full rank, i.e.,  $\text{rank}(\bar{A}_G) = |V|$ , then system (1) has a unique solution. A standard method, like the Gauss-Jordan elimination, can be used to uncover  $\ell$  without any surgical probe in polynomial time.

## 42:6 The Generalized Microscopic Image Reconstruction Problem

If  $\text{rank}(\bar{A}_G) < |V|$ , then system (1) has (infinitely) many solutions. The column space  $C(\bar{A}_G)$  of  $\bar{A}_G$  contains all vectors  $\bar{A}_G \cdot x$ . It is spanned by a maximal subset of independent columns of  $\bar{A}_G$ , and its dimension is  $\text{rank}(\bar{A}_G)$ . The kernel  $\ker(\bar{A}_G)$  of  $\bar{A}_G$  consists of all solutions to the homogeneous system  $\bar{A}_G \cdot x = 0$ ; its dimension is  $s \triangleq |V| - \text{rank}(\bar{A}_G)$ . To describe all solutions of system (1), let  $x$  be a vector such that  $\bar{A}_G \cdot x = \mathcal{P}$ . Then,

$$\bar{A}_G \cdot (x + x_0) = \bar{A}_G \cdot x + \bar{A}_G \cdot x_0 = \mathcal{P} + 0 = \mathcal{P}$$

for any  $x_0 \in \ker(\bar{A}_G)$ .

To uncover  $\ell$ , we need to remove this ambiguity by surgical probes. One approach is to select a maximal subset of independent columns  $U$  of  $\bar{A}_G$ . The columns of  $U$  are a basis of  $C(\bar{A}_G)$ , and  $|U| = \text{rank}(\bar{A}_G)$ . Let  $U' = \bar{A}_G \setminus U$  be the remaining columns. Thus,  $|U'| = s$ . Probing the vertices that correspond to the columns of  $U'$  returns  $\bar{\ell} \in \mathbb{R}^s$ . Now, we can solve the system

$$U \cdot x = \mathcal{P} - U' \cdot \bar{\ell} \tag{2}$$

to uncover the unknown entries of  $\ell$ . If  $\ell$  is a solution of system (1), then system (2) has at least one solution. Since  $U$  is a set of linearly independent columns, this solution is unique. If we select more than  $\text{rank}(\bar{A}_G)$  columns to form  $U$ , system (2) does not have a unique solution.

A structured way to select a maximal subset of independent columns of  $\bar{A}_G$  is the *reduced row echelon form*. The reduced row echelon form can be computed in polynomial time using the Gauss-Jordan elimination method (cf. [11]). The output is a partition of the columns into *pivot-columns* and *free-columns*. The pivot-columns form a basis of  $C(\bar{A}_G)$ . We probe the vertices corresponding to the free-columns. Back-substitution takes care of uncovering the missing entries of  $\ell$  (if  $\bar{A}_G$  was augmented by  $\mathcal{P}$  before the elimination process). ◀

Note that the rank of  $\bar{A}_G$  can be as low as one, e.g., in the case of the complete graph  $K_n$  we have  $\text{rank}(\bar{A}_{K_n}) = 1$ . Hence, to solve MINIMUM SURGICAL PROBING for  $K_n$  a maximum number of  $n - 1$  surgical probes is required. However, as we will see in the following sections, there are many graphs for which we can uncover  $\ell$  without any surgical probes.

In classic DTR problems the labels are binary or integer vectors. If we add respective constraints on  $\ell$  to System (1), Theorem 2 provides an upper bound on the number of required surgical probes.

### 3 Minimum Surgical Probing in Trees

In this section we consider the MINIMUM SURGICAL PROBING problem in trees. A first class of trees that requires no surgical probes are stars.

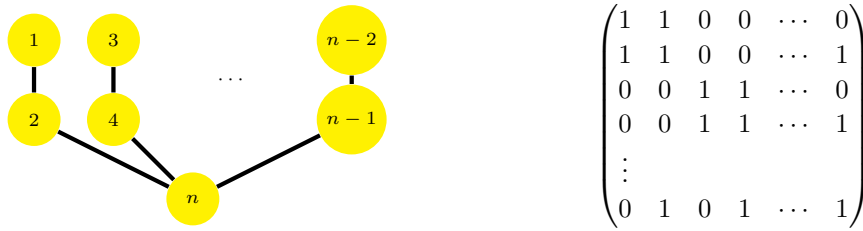
► **Lemma 3.** *A star graph requires no surgical probes to uncover  $\ell$ .*

**Proof.** Let  $G$  be a star with  $n \geq 3$  vertices  $\{1, \dots, n\}$  where vertex  $n$  is the center. The label  $\ell_n$  can be computed from the neighborhood probes as follows:

$$\frac{1}{n-2}(\sum_{i=1}^{n-1} \mathcal{P}_i - \mathcal{P}_n) = \frac{1}{n-2}(\sum_{i=1}^{n-1} (\ell_n + \ell_i) - (\ell_n + \sum_{i=1}^{n-1} \ell_i)) = \ell_n .$$

Given  $\ell_n$ , the remaining labels can be computed using  $\ell_i = \mathcal{P}_i - \ell_n$ , for  $i < n$ . ◀

The following theorem shows an upper bound on the number of surgical probes that are required to uncover bipartite graphs. Trees are always connected and bipartite.



(a) Spider with  $\frac{n-1}{2}$  legs.

(b) Adj. matrix of a spider.

■ **Figure 2** A spider graph and its adjacency matrix.

► **Theorem 4.** *Let  $G = (L \cup R, E)$  be a connected, bipartite graph with  $n \geq 3$  nodes. Then  $\ell$  can be uncovered using  $\lfloor \frac{n}{2} \rfloor - 1$  many surgical probes.*

**Proof.** Assume without loss of generality that  $|L| \leq |R|$ . Observe that there must be a node  $v \in L$  such that  $\text{deg}(v) > 1$  since  $G$  is connected. Now, surgical probe  $L \setminus \{v\}$  and uncover the labels of all nodes in  $R \setminus N(v)$ . This can be done since the induced graph  $T[(L \setminus \{v\}) \cup (R \setminus N(v))]$  is bipartite and we know all the labels of one of the blocks. Since the graph that is induced by the nodes with unknown labels is a star, we are done due to Lemma 3.

If  $n$  is even, we perform at most  $\frac{n}{2} - 1 = \frac{n-2}{2}$  many surgical probes. If  $n$  is odd, we perform at most  $\frac{n-1}{2} - 1 = \frac{n-3}{2}$  many surgical probes. ◀

We can show that the given upper bound is tight for trees where the number of vertices is odd.

► **Theorem 5.** *There exist  $n$ -vertex trees, for odd  $n$ , that require  $\lfloor \frac{n}{2} \rfloor - 1$  surgical probes.*

**Proof.** Consider a spider  $G$  with  $\frac{n-1}{2}$  legs as shown in Figure 2a. The adjacency matrix is given in Figure 2b. Elementary row operations can be used to show that  $\text{rank}(\bar{A}_G) = \frac{n+3}{2}$ . To see this, subtract each odd row  $i < n$  from its succeeding row  $i + 1$ . The claim follows from Theorem 2. ◀

Another class of trees that require no surgical probes are perfect  $k$ -ary trees. Recall that a perfect  $k$ -ary tree is a tree where all internal nodes have  $k$  children and all leaves have the same depth.

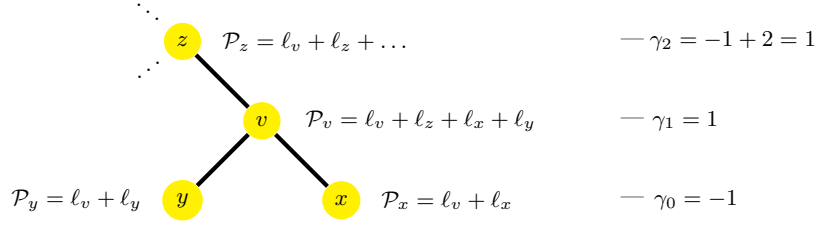
► **Theorem 6.** *Let  $T = (V, E)$  be a perfect  $k$ -ary tree. Then, no surgical probes are needed to uncover  $\ell$ .*

**Proof.** We prove the theorem by induction on the height  $h$  of  $T$ . For a vertex  $v$  we denote the set of its children by  $ch(v)$ . As a base case, we consider  $h = 1$ . This yields a  $(k + 1)$ -vertex star graph, and due to Lemma 3, no surgical probes are needed to uncover  $\ell$ .

Now, let  $h \geq 2$  and let  $r$  be the root of  $T$ . We start by calculating the root label,  $\ell_r$ , based on the given neighborhood probes. To do that, we express  $\ell_r$  as a function of the probe results over the entire tree. This is done as follows. Arrange the tree vertices in levels, with the leaves on level 0 and the root  $r$  on level  $h$ . Let

$$\gamma_j = \begin{cases} -1 & j = 0, \\ 1 & j = 1, \\ -\gamma_{j-1} - k \cdot \gamma_{j-2} & j \geq 2, \end{cases} \quad \text{and} \quad b = \gamma_h + k \cdot \gamma_{h-1}. \quad (3)$$

Next, define a coefficient  $a_v = \gamma_j$  for every vertex  $v$  on level  $j$ .



■ **Figure 3** Part of a perfect binary tree. Vertices  $x$  and  $y$  are leaves. The label  $l_x$  appears only in  $\mathcal{P}_x$  and  $\mathcal{P}_v$ . Their coefficients sum up to 0, i.e., the label cancels out. Analogously, the labels  $l_y$  and  $l_v$  cancel out.

▷ **Claim 7.** The root label satisfies 
$$b \cdot \ell_r = \sum_{v \in V} a_v \mathcal{P}_v .$$

Proof. Consider the sum on the right hand side. Observe that for every vertex  $v$  except the root  $r$ , the contribution of the label  $l_v$  to this sum is cancelled out. To see this, note the following observations:

- The label of a leaf  $v$  appears once in  $\mathcal{P}_v$  and once in  $\mathcal{P}_z$  where  $z$  is  $v$ 's parent, so it is cancelled out in the sum since the coefficients of these probes are  $a_v = -1$  and  $a_z = 1$ .
- The label of a nonleaf  $v$  on level 1 appears in  $\mathcal{P}_v$ ,  $\mathcal{P}_z$ , and  $\mathcal{P}_x$  for  $x \in ch(v)$  where  $z$  is  $v$ 's parent, so it is cancelled out since the coefficients of these probes are  $a_x = -1$  ( $k$  times in the sum),  $a_v = 1$ , and  $a_z = k - 1$ .
- The label of a vertex  $v$  on level  $2 \leq j < h$  appears in  $\mathcal{P}_v$ ,  $\mathcal{P}_z$ , and  $\mathcal{P}_x$  for  $x \in ch(v)$  where  $z$  is  $v$ 's parent, so it is cancelled out in the sum since the coefficients of these probes are  $a_x = \gamma_{j-1}$  ( $k$  times in the sum),  $a_v = -\gamma_{j-1} - k \cdot \gamma_{j-2}$ , and  $a_z = -\gamma_j - k \cdot \gamma_{j-1} = -(-\gamma_{j-1} - k \cdot \gamma_{j-2}) - k \cdot \gamma_{j-1} = -(k-1) \cdot \gamma_{j-1} + k \cdot \gamma_{j-2}$ .

See Figure 3 for an example of a perfect 2-ary (binary) tree.

It follows that the only label that remains in the sum is the root label  $\ell_r$ . This label appears in  $\mathcal{P}_r$  and  $\mathcal{P}_x$  for  $x \in ch(r)$ . The coefficients of these probes are  $a_x = \gamma_{h-1}$  and  $a_r = \gamma_h$ . Hence, after all other labels are canceled out, the sum simplifies to  $(\gamma_h + k \cdot \gamma_{h-1})\ell_r = b\ell_r$ .  $\triangleleft$

▷ **Claim 8.**  $b \neq 0$ .

Proof. By Eq. (3),  $b = -\gamma_{h+1}$ . The recursion of Eq. (3) solves to the following explicit formula<sup>2</sup>:

$$\gamma_j = \frac{2^{-j-1}}{\sqrt{1-4 \cdot k}} \cdot \left( (-1 - \sqrt{1-4 \cdot k})^{j+1} - (-1 + \sqrt{1-4 \cdot k})^{j+1} \right) .$$

Hence  $b = -\gamma_{h+1} = 0$  if and only if  $-\sqrt{1-4 \cdot k} = \sqrt{1-4 \cdot k}$ , which is false.  $\triangleleft$

Claims 7 and 8 enable us to extract  $\ell_r$  from the neighborhood probes  $\mathcal{P}$  without using any surgical probes. Subsequently, we use the inductive argument to calculate the rest of the labels, proving the claim for  $h$ . To do this, we remove  $r$  from the tree  $T$ , and get  $k$  smaller trees  $T_i$  whose roots are  $r_i$  for  $i \in [k]$ . As the trees  $T_i$  are trees of height  $h-1$ , we can use the inductive hypothesis to solve for  $\ell$  on each of the subtrees  $T_i$ . The only correction required is that before solving the labels on the subtrees  $T_i$ , we need to fix the probe results on the

<sup>2</sup> the explicit formula can be computed with a computer algebra system



roots,  $r_i$ , since probing the vertex  $r_i$  in  $T_i$  yields a different value than in  $T$  (in which  $r_i$  has another neighbor,  $r$ ). Hence, to get the correct labels of these roots in  $T_i$ , we need to subtract  $\ell_r$  from  $\mathcal{P}_{r_i}$ . More precisely, for  $i \in [k]$ , let us denote by  $\hat{\mathcal{P}}_{r_i}$  the expected outcome of the probe operation on  $r_i$  had it been applied to the tree  $T_i$ . Then  $\hat{\mathcal{P}}_{r_i} = \mathcal{P}_{r_i} - \ell_r$ . ◀

## 4 Mesh graphs and Cartesian Products

In this section we consider mesh graphs, which are Cartesian products of simpler graphs. For example, grid graphs which were studied in previous papers on discrete tomography can be presented as the Cartesian product of two path graphs. In addition to grid graphs, we consider the Cartesian product of a path and a cycle (a tube) and two cycles (a torus).

**Graph Products.** Let us start with some definitions and notation, following [5]. Given two graphs,  $G_1 = (V_1, E_1)$  and  $G_2 = (V_2, E_2)$ , the *Cartesian product* of  $G_1$  and  $G_2$ , denoted  $G_1 \square G_2$ , is the graph  $G = (V, E)$  where  $V = V_1 \times V_2$  and

$$E = \{(v, u), (v', u) : (v, v') \in E_1\} \cup \{(v, u), (v, u') : (u, u') \in E_2\} .$$

The adjacency matrices of the path and cycle graphs are connected to the product graphs' adjacency matrices by the Kronecker product and Kronecker sum. Given two square matrices  $A$  and  $B$  of respective sizes  $n$  and  $m$ , the *Kronecker product* and *Kronecker sum* of  $A$  and  $B$  are defined, respectively, as

$$A \otimes B \triangleq [a_{ij} \bar{B}] \quad \text{and} \quad A \oplus B \triangleq (A \otimes I_m) + (I_n \otimes B) .$$

The Kronecker sum of the adjacency matrices of two graphs is the adjacency matrix of the Cartesian product graph, i.e.,  $A_{G_1 \square G_2} = (A_{G_1} \otimes I_{|V_2|}) + (I_{|V_1|} \otimes A_{G_2})$ .

The Kronecker sum preserves eigenvalues of its summands in the following way.

► **Theorem 9** ([5]). *Let  $G_1$  and  $G_2$  be graphs. Then, the set of eigenvalues of  $A_{G_1 \square G_2}$  is the Minkowski sum of the set of eigenvalues of  $A_{G_1}$  and the set of eigenvalues of  $A_{G_2}$ , i.e., it is*

$$\Lambda(A_{G_1 \square G_2}) = \{\lambda + \mu \mid \lambda \in \Lambda(A_{G_1}), \mu \in \Lambda(A_{G_2})\} .$$

**Cosine at Rational Angles.** The required number of surgical probes for the graphs studied herein is determined by the number of solutions to equations that involve trigonometric functions. In particular, rational values of the cosine function at rational angles are of interest. A rational angle is a rational multiple of  $\pi$ . Conway and Jones [6] give a characterization of linear combinations of up to four cosine functions at rational angles that are rational.

► **Theorem 10** ([6]). *Suppose we have at most four distinct rational multiples of  $\pi$  lying strictly between 0 and  $\frac{\pi}{2}$  for which some rational linear combination of their cosines is rational but no proper subset has this property. Then the appropriate linear combination is proportional to one from the following list:*

- $\cos(\frac{\pi}{3}) = \frac{1}{2}$
- $-\cos(\varphi) + \cos(\frac{\pi}{3} - \varphi) + \cos(\frac{\pi}{3} + \varphi) = 0 \quad (0 < \varphi < \frac{\pi}{6})$
- $\cos(\frac{\pi}{5}) - \cos(\frac{2\pi}{5}) = \frac{1}{2}$
- $\cos(\frac{\pi}{7}) - \cos(\frac{2\pi}{7}) + \cos(\frac{3\pi}{7}) = \frac{1}{2}$
- $\cos(\frac{\pi}{5}) - \cos(\frac{\pi}{15}) + \cos(\frac{4\pi}{15}) = \frac{1}{2}$
- $-\cos(\frac{2\pi}{5}) + \cos(\frac{2\pi}{15}) - \cos(\frac{7\pi}{15}) = \frac{1}{2}$
- $\cos(\frac{\pi}{7}) + \cos(\frac{3\pi}{7}) - \cos(\frac{\pi}{21}) + \cos(\frac{8\pi}{21}) = \frac{1}{2}$

## 42:10 The Generalized Microscopic Image Reconstruction Problem

- $-\cos(\frac{2\pi}{7}) + \cos(\frac{3\pi}{7}) + \cos(\frac{4\pi}{21}) + \cos(\frac{10\pi}{21}) = \frac{1}{2}$
- $\cos(\frac{\pi}{7}) - \cos(\frac{2\pi}{7}) + \cos(\frac{2\pi}{21}) - \cos(\frac{5\pi}{21}) = \frac{1}{2}$
- $-\cos(\frac{\pi}{15}) + \cos(\frac{2\pi}{15}) + \cos(\frac{4\pi}{15}) - \cos(\frac{7\pi}{15}) = \frac{1}{2}$

The angles are normalized due to the symmetry of the cosine function. The theorem does not cover the values of the cosine function at 0 and multiples of  $\frac{\pi}{2}$ . This is characterized by the following theorem.

► **Theorem 11** ([13]). *The only rational values of the circular trigonometric functions at rational multiples of  $\pi$  are 0,  $\pm\frac{1}{2}$  and  $\pm 1$  for cosine and sine, 0 and  $\pm 1$  for tangent and cotangent, and  $\pm 1$  and  $\pm 2$  for secant and cosecant.*

**Grids and Paths.** We exploit the fact that mesh graphs are products of simpler graphs to determine the number of surgical probes without having to resort to Theorem 2.

► **Theorem 12.** *Let  $G$  be a grid graph of size  $n_1 \times n_2$ . The number of surgical probes that are sufficient to uncover  $\ell$  is*

$$\mathcal{I}_1^2(n_1)\mathcal{I}_2^3(n_2) + \mathcal{I}_2^3(n_1)\mathcal{I}_1^2(n_2) + 2\mathcal{I}_4^5(n_1)\mathcal{I}_4^5(n_2).$$

*In particular, the number of surgical probes to uncover  $\ell$  for grid graphs of any size is at most 4.*

**Proof.** Let  $G$  be a grid graph which is the Cartesian product of the two path graphs  $P_1$  and  $P_2$ , of length  $n_1$  and  $n_2$ , resp. By Lemma 1, we look for eigenvalues of  $A_G$  that are  $-1$ . By Theorem 9, we need to identify eigenvalues of  $A_{P_1}$  and  $A_{P_2}$  that add up to  $-1$ . The eigenvalues of  $A_P$  where  $P$  is a path of length  $n$  are given by  $2\cos(\frac{\pi j}{n+1})$ , for  $j \in [1, n]$  (cf. [5]). Hence, we are looking for the number of solutions to the following equation:

$$2\cos\left(\frac{i}{n_1+1} \cdot \pi\right) + 2\cos\left(\frac{j}{n_2+1} \cdot \pi\right) = -1, \quad (4)$$

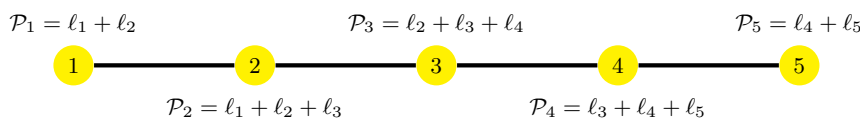
for  $i \in [1, n_1]$  and  $j \in [1, n_2]$ .

Due to Theorem 11 the only rational values the cosine function takes at rational angles are 0,  $\pm\frac{1}{2}$  and  $\pm 1$ . Since  $0 < \frac{i}{n_1+1}, \frac{j}{n_2+1} < 1$ , the values 0 and  $-\frac{1}{2}$  are the only combination that can satisfy Eq. (4). For  $0 < x < 1$ , the equations  $\cos(\pi x) = 0$  and  $\cos(\pi x) = -\frac{1}{2}$  have solutions  $x = \frac{1}{2}$  and  $x = \frac{2}{3}$ , respectively. Hence, Eq. (4) has a solution if  $3i = 2(n_1 + 1)$  and  $2j = n_2 + 1$ . This is the case if  $n_1 \bmod 3 \equiv 2$  and  $n_2 \bmod 2 \equiv 1$ . Here, we have that  $\frac{2(n_1+1)}{3} \in [1, n_1]$  and  $\frac{n_2+1}{2} \in [1, n_2]$ . Due to symmetry, we get another solution if  $n_1 \bmod 2 \equiv 1$  and  $n_2 \bmod 3 \equiv 2$ .

Theorem 10 characterizes linear combinations of cosine functions that have a rational value. Here, the values of a single cosine function are irrational. For a combination of two cosine functions, Theorem 10 states that there is only one such combination:  $\cos(\frac{\pi}{5}) - \cos(\frac{2\pi}{5}) = \frac{1}{2}$ . Due to symmetry,  $\cos(\frac{\pi}{5}) = -\cos(\frac{4\pi}{5})$ , and we derive

$$2\cos\left(\frac{4\pi}{5}\right) + 2\cos\left(\frac{2\pi}{5}\right) = -1. \quad (5)$$

Hence, Eq. (4) has a solution if  $5i = 4(n_1 + 1)$  and  $5j = 2(n_2 + 1)$ . For  $4(n_1 + 1)$  or  $2(n_2 + 1)$  to become a multiple of 5, we need that  $n_1 \bmod 5 \equiv 4$  and  $n_2 \bmod 5 \equiv 4$ . In both cases,  $\frac{4(n_1+1)}{5}, \frac{2(n_1+1)}{5} \in [1, n_1]$  and  $\frac{4(n_2+1)}{5}, \frac{2(n_2+1)}{5} \in [1, n_2]$  giving two solutions to Eq. (4) if both  $n_1 \bmod 5 \equiv 4$  and  $n_2 \bmod 5 \equiv 4$ . ◀



■ **Figure 4** A path of length  $n = 5$ . One probe is needed, but not at  $i = 3$ .

There are many grids where no surgical probes are required to uncover  $\ell$  (e.g. the  $3 \times 3$  grid). In the worst case, a total of 4 surgical probes is required to uncover  $\ell$ . This is the case if  $n_1 = 30i - 1$  and  $n_2 = 30j - 1$ , for  $i, j \in \mathbb{N}$ .

When  $n_2 = 1$ , i.e., graph  $G$  is a path, we can also provide a linear time algorithm for uncovering  $\ell$ .

► **Theorem 13.** *Let  $P$  be a path with  $n$  vertices, where  $V = \{1, \dots, n\}$ . If  $n \bmod 3 \equiv 2$ , then a single probe is needed, and it should be at a node  $i$  such that  $i \bmod 3 \neq 0$ . Otherwise, no surgical probes are needed. In both cases, the labels can be discovered in  $O(n)$  time.*

**Proof.** The number of surgical probes follows from Theorem 12

To discover the labels along the path, we use the following procedure. First, the label  $\ell_3$  can be discovered using  $\ell_3 = \mathcal{P}_2 - \mathcal{P}_1$ . Iteratively,  $\ell_{3i}$ , for  $i = 2, \dots, \lfloor \frac{n}{3} \rfloor$ , can be discovered using

$$\mathcal{P}_{3i-1} - \mathcal{P}_{3i-2} + \ell_{3i-3} = (\ell_{3i-2} + \ell_{3i-1} + \ell_{3i}) - (\ell_{3i-3} + \ell_{3i-2} + \ell_{3i-1}) + \ell_{3i-3} = \ell_{3i} .$$

If  $n \bmod 3 \neq 2$ , we discover either  $\ell_n$  or  $\ell_{n-1}$  in the last iteration. We may discover the other value due to  $\mathcal{P}_n = \ell_{n-1} + \ell_n$ . Given  $\ell_n$  and  $\ell_{n-1}$ , we may discover the rest of the labels going from right to left. If  $n \bmod 3 \equiv 2$ , then probe any vertex  $i \in [n]$ , such that  $i \bmod 3 \neq 2$ . The probe splits the path into two sub-paths of length  $n_1$  and  $n_2$ , where  $n_1, n_2 \bmod 3 \neq 2$ . The rest of the labels can be discovered as above, for each sub-path. See Figure 4. ◀

**Tubes and Cycles.** A tube graph is a Cartesian product of a path and a cycle graph. We denote the length of the path by  $n_1$  and the length of the cycle by  $n_2 \geq 3$ .

► **Theorem 14.** *Let  $T$  be a tube graph of dimensions  $n_1 \times n_2$ . The number of surgical probes that are sufficient to uncover  $\ell$  is*

$$2\mathcal{I}_1^2(n_1)\mathcal{I}_0^3(n_2) + \mathcal{I}_2^3(n_1)\mathcal{I}_0^2(n_2) + 2\mathcal{I}_2^3(n_1)\mathcal{I}_0^4(n_2) + 4\mathcal{I}_4^5(n_1)\mathcal{I}_0^5(n_2).$$

*In particular, the number of surgical probes to uncover  $\ell$  for any tube graph is at most 9.*

**Proof.** Let  $T$  be a tube graph which is the Cartesian product of a path graphs  $P$  and a cycle  $C$ , of length  $n_1$  and  $n_2$ , resp. The eigenvalues of  $A_P$  are given by  $2 \cos(\frac{\pi i}{n_1+1})$ , for  $i \in [1, n_1]$ , and the eigenvalues of  $A_C$  are given by  $2 \cos(\frac{2\pi j}{n_2})$ , for  $j \in [0, n_2 - 1]$  (cf. [5]). By Theorem 9 and Lemma 1, we are interested in solutions of the equation

$$2 \cos\left(\frac{i}{n_1+1} \cdot \pi\right) + 2 \cos\left(\frac{2j}{n_2} \cdot \pi\right) = -1. \tag{6}$$

Since  $0 < \frac{\pi i}{n_1+1} < \pi$ ,  $\cos(\frac{\pi i}{n_1+1})$  has the rational values  $-\frac{1}{2}, 0, \frac{1}{2}$ , and since  $0 \leq \frac{2\pi j}{n_2} < 2\pi$ ,  $\cos(\frac{2\pi j}{n_2})$ , has the rational values  $-1, -\frac{1}{2}, 0, \frac{1}{2}, 1$ , due to Theorem 11. This gives us the solutions to Eq. (6) where both cosine functions have rational values. The following combinations satisfy Eq. (6):

## 42:12 The Generalized Microscopic Image Reconstruction Problem

- $\cos(\frac{\pi i}{n_1+1}) = -\frac{1}{2}$  and  $\cos(\frac{2\pi j}{n_2}) = 0$ . The equation  $\cos(\pi x) = -\frac{1}{2}$  has one solution  $x = \frac{2}{3}$ , for  $0 < x < 1$ . Our question is reduced to  $3i = 2(n_1 + 1)$ . For  $2(n_1 + 1)$  to become a multiple of 3, we need that  $n_1 \bmod 3 \equiv 2$ . In this case,  $\frac{2}{3}(n_1 + 1) \in [1, n_1]$ . The equation  $\cos(2\pi x) = 0$  has two solutions  $x = \frac{1}{4}$  and  $x = \frac{3}{4}$ , for  $0 \leq x < 1$ . Hence, either  $4j = n_2$  or  $4j = 3n_2$ . It follows that if  $n_2$  is a multiple of 4, we have that  $\frac{n_2}{4}, \frac{3n_2}{4} \in [0, n_2 - 1]$ . We get two solutions for Eq. (6) if  $n_1 \bmod 3 \equiv 2$  and  $n_2 \bmod 4 \equiv 0$ .
- $\cos(\frac{\pi i}{n_1+1}) = 0$  and  $\cos(\frac{2\pi j}{n_2}) = -\frac{1}{2}$ . The equation  $\cos(\pi x) = 0$  has one solution  $x = \frac{1}{2}$ , for  $0 < x < 1$ . Our question is reduced to  $2i = n_1 + 1$ . For  $n_1 + 1$  to become a multiple of 2, we need that  $n_1 \bmod 2 \equiv 1$ . In this case,  $\frac{1}{2}(n_1 + 1) \in [1, n_1]$ . The equation  $\cos(2\pi x) = -\frac{1}{2}$  has two solutions  $x = \frac{1}{3}$  and  $x = \frac{2}{3}$ , for  $0 \leq x < 1$ . Hence, either  $3j = n_2$  or  $3j = 2n_2$ . It follows that if  $n_2$  is a multiple of 3, we have that  $\frac{n_2}{3}, \frac{2n_2}{3} \in [0, n_2 - 1]$ . We get two solutions for Eq. (6) if  $n_1 \bmod 2 \equiv 1$  and  $n_2 \bmod 3 \equiv 0$ .
- $\cos(\frac{\pi i}{n_1+1}) = \frac{1}{2}$  and  $\cos(\frac{2\pi j}{n_2}) = -1$ . The equation  $\cos(\pi x) = \frac{1}{2}$  has one solution  $x = \frac{1}{3}$ , for  $0 < x < 1$ . Our question is reduced to  $3i = n_1 + 1$ . For  $n_1 + 1$  to become a multiple of 3, we need that  $n_1 \bmod 3 \equiv 2$ . In this case,  $\frac{1}{3}(n_1 + 1) \in [1, n_1]$ . The equation  $\cos(2\pi x) = -1$  has one solution  $x = \frac{1}{2}$ , for  $0 \leq x < 1$ . Hence, we need that  $2j = n_2$ . It follows that if  $n_2$  is a multiple of 2, we have that  $\frac{n_2}{2} \in [0, n_2 - 1]$ . We get one solution for Eq. (6) if  $n_1 \bmod 3 \equiv 2$  and  $n_2 \bmod 2 \equiv 0$ .

Theorem 10 characterizes a linear combination of two cosines which yields four more solutions to Eq. (6). We derive Eq. (5) again:  $2 \cos(\frac{4\pi}{5}) + 2 \cos(\frac{2\pi}{5}) = -1$ . We have  $\cos(\frac{4\pi}{5}) = \frac{1}{4}(-1 - \sqrt{5})$ . The equation  $\cos(\pi x) = \frac{1}{4}(-1 - \sqrt{5})$  has one solution  $x = \frac{4}{5}$ , for  $0 < x < 1$ . Our question is reduced to  $5i = 4(n_1 + 1)$ . For  $n_1 + 1$  to become a multiple of 5, we need that  $n_1 \bmod 5 \equiv 4$ . In this case,  $\frac{4}{5}(n_1 + 1) \in [1, n_1]$ . We have  $\cos(\frac{2\pi}{5}) = \frac{1}{4}(-1 + \sqrt{5})$ . The equation  $\cos(2\pi x) = \frac{1}{4}(-1 + \sqrt{5})$  has two solutions  $x = \frac{1}{5}$  and  $x = \frac{4}{5}$ , for  $0 \leq x < 1$ . Hence, either  $5j = n_2$  or  $5j = 4n_2$ . It follows that if  $n_2$  is a multiple of 5, we have that  $\frac{2n_2}{5}, \frac{4n_2}{5} \in [0, n_2 - 1]$ . We get two solutions for Eq. (6) if  $n_1 \bmod 5 \equiv 4$  and  $n_2 \bmod 5 \equiv 0$ .

Since  $n_1$  and  $n_2$  can switch, we get another pair of solutions. The equation  $\cos(\pi x) = \frac{1}{4}(-1 + \sqrt{5})$  has one solution  $x = \frac{2}{5}$ , for  $0 < x < 1$ . Our question is reduced to  $5i = 2(n_1 + 1)$ . For  $n_1 + 1$  to become a multiple of 5, we need that  $n_1 \bmod 5 \equiv 4$ . In this case,  $\frac{4}{5}(n_1 + 1) \in [1, n_1]$ . We have  $\cos(\frac{2\pi}{5}) = \frac{1}{4}(-1 + \sqrt{5})$ . The equation  $\cos(2\pi x) = \frac{1}{4}(-1 - \sqrt{5})$  has two solutions  $x = \frac{2}{5}$  and  $x = \frac{3}{5}$ , for  $0 \leq x < 1$ . Hence, either  $5j = 2n_2$  or  $5j = 3n_2$ . It follows that if  $n_2$  is a multiple of 5, we have that  $\frac{2n_2}{5}, \frac{3n_2}{5} \in [0, n_2 - 1]$ . In summary, we get four solutions for Eq. (6) if  $n_1 \bmod 5 \equiv 4$  and  $n_2 \bmod 5 \equiv 0$ . ◀

► **Theorem 15.** *Let  $C$  be a cycle of length  $n$ . If  $n \bmod 3 \equiv 0$ , then two probes are needed, and they should be at nodes  $i, j$  such that  $i - j \bmod 3 \not\equiv 0$ . Otherwise, no surgical probes are needed. In both cases, the labels can be discovered in  $O(n)$  time.*

**Proof.** The number of surgical probes follows from Theorem 14

To discover the labels of a cycle, we use the following

- If  $n \bmod 3 \equiv 0$ , then probe vertex 1 which can be understood as removing the vertex from the cycle. Hence, we are left with a path of length  $n - 1$ . Since  $(n - 1) \bmod 3 \equiv 2$ , we can use the procedure described in the proof of Theorem 13 to discover the remaining labels with one additional surgical probe.

- If  $n \bmod 3 \equiv 1$ , we compute  $\ell_1$  as follows:

$$\begin{aligned} 3\ell_1 &= (\ell_n + \ell_1 + \ell_2) + \sum_{i=1}^{\lfloor n/3 \rfloor} (\ell_{3i-2} - \ell_{3i-1} - \ell_{3i+1} + \ell_{3i+2}) \\ &= \mathcal{P}_1 + \sum_{i=1}^{\lfloor n/3 \rfloor} (\mathcal{P}_{3i-1} - 2\mathcal{P}_{3i} + \mathcal{P}_{3i+1}) . \end{aligned}$$

- If  $n \bmod 3 \equiv 2$ , we compute  $\ell_1$  as follows:

$$\begin{aligned} 3\ell_1 &= (-\ell_n + \ell_1 + \ell_2 + 2\ell_3) + \sum_{i=1}^{\lfloor n/3 \rfloor} (-\ell_{3i-1} - 2\ell_{3i} + \ell_{3i+2} + 2\ell_{3i+3}) \\ &= -\mathcal{P}_1 + 2\mathcal{P}_2 + \sum_{i=1}^{\lfloor n/3 \rfloor} (-\mathcal{P}_{3i} - \mathcal{P}_{3i+1} + 2\mathcal{P}_{3i+2}) . \end{aligned}$$

In the two latter cases we are left with a path where we can uncover the remaining labels without any surgical probes due to Theorem 13. ◀

**Tori.** A *torus* graph is a Cartesian product of two cycle graphs.

► **Theorem 16.** *Let  $T$  be a torus graph of dimensions  $n_1 \times n_2$ . The number of surgical probes that are sufficient to uncover  $\ell$  is*

$$4\mathcal{I}_0^3(n_1)\mathcal{I}_0^4(n_2) + 4\mathcal{I}_0^4(n_1)\mathcal{I}_0^3(n_2) + 2\mathcal{I}_0^2(n_1)\mathcal{I}_0^6(n_2) + 2\mathcal{I}_0^6(n_1)\mathcal{I}_0^2(n_2) + 8\mathcal{I}_0^5(n_1)\mathcal{I}_0^5(n_2).$$

In particular, the number of surgical probes to uncover  $\ell$  for any torus graph is at most 20.

**Proof.** Let  $T$  be a torus graph which is the Cartesian product of two cycles  $C_1$  and  $C_2$  of lengths  $n_1$  and  $n_2$ , resp. The eigenvalues of  $A_{C_i}$  are given by  $2 \cos(\frac{2j\pi}{n_i})$ , for  $j \in [0, n_i - 1]$  (cf. [5]). By Theorem 9 and Lemma 1, we are interested in solutions of the equation

$$2 \cos\left(\frac{2i}{n_1} \cdot \pi\right) + 2 \cos\left(\frac{2j}{n_2} \cdot \pi\right) = -1 . \tag{7}$$

The two summands  $\cos(\frac{2i\pi}{n_1})$  and  $\cos(\frac{2j\pi}{n_2})$  have the rational values  $-1, -\frac{1}{2}, 0, \frac{1}{2}, 1$ , due to Theorem 11. This gives us the solutions to Eq. (6) where both cosine functions have rational values. We consider the combinations that satisfy Eq. (7):

- $\cos(\frac{2i\pi}{n_1}) = -\frac{1}{2}$  and  $\cos(\frac{2j\pi}{n_2}) = 0$ . The equation  $\cos(2\pi x) = -\frac{1}{2}$  has two solutions  $x = \frac{1}{3}$  and  $x = \frac{2}{3}$ , for  $0 \leq x < 1$ . It follows that if  $n_1$  is a multiple of 3, we have that  $\frac{n_1}{3}, \frac{2n_1}{3} \in [0, n_1 - 1]$ . The equation  $\cos(2\pi x) = 0$  has two solutions  $x = \frac{1}{4}$  and  $x = \frac{3}{4}$ , for  $0 \leq x < 1$ . It follows that if  $n_2$  is a multiple of 4, we have that  $\frac{n_2}{4}, \frac{3n_2}{4} \in [0, n_2 - 1]$ . We get four solutions for Eq. (7) if  $n_1 \bmod 3 \equiv 0$  and  $n_2 \bmod 4 \equiv 0$ .
- $\cos(\frac{2i\pi}{n_1}) = 0$  and  $\cos(\frac{2j\pi}{n_2}) = -\frac{1}{2}$ . Similarly, we get four solutions if  $n_1 \bmod 4 \equiv 0$  and  $n_2 \bmod 3 \equiv 0$ .
- $\cos(\frac{2i\pi}{n_1}) = \frac{1}{2}$  and  $\cos(\frac{2j\pi}{n_2}) = -1$ . The equation  $\cos(2\pi x) = \frac{1}{2}$  has two solutions  $x = \frac{1}{6}$  and  $x = \frac{5}{6}$ , for  $0 \leq x < 1$ . It follows that if  $n_1$  is a multiple of 6, we have that  $\frac{n_1}{6}, \frac{5n_1}{6} \in [0, n_1 - 1]$ . The equation  $\cos(2\pi x) = -1$  has one solution  $x = \frac{1}{2}$ , for  $0 \leq x < 1$ . It follows that if  $n_2$  is a multiple of 2, we have that  $\frac{n_2}{2} \in [0, n_2 - 1]$ . We get two solutions for Eq. (7) if  $n_1 \bmod 2 \equiv 0$  and  $n_2 \bmod 6 \equiv 0$ .
- $\cos(\frac{2i\pi}{n_1}) = -1$  and  $\cos(\frac{2j\pi}{n_2}) = \frac{1}{2}$ . Similarly, we get two solutions if  $n_1 \bmod 6 \equiv 0$  and  $n_2 \bmod 2 \equiv 0$ .

Theorem 10 characterizes a linear combination of two cosines which yields eight more solutions to Eq. (7). We derive Eq. (5) once again:  $2 \cos\left(\frac{4\pi}{5}\right) + 2 \cos\left(\frac{2\pi}{5}\right) = -1$ . We have  $\cos\left(\frac{4\pi}{5}\right) = -\frac{1+\sqrt{5}}{4}$ . The equation  $\cos(2\pi x) = -\frac{1+\sqrt{5}}{4}$  has two solutions  $x = \frac{2}{5}$  and  $x = \frac{3}{5}$ , for  $0 \leq x < 1$ . It follows that if  $n_1$  is a multiple of 5, we have that  $\frac{2n_1}{5}, \frac{3n_1}{5} \in [0, n_1 - 1]$ . We have  $\cos\left(\frac{2\pi}{5}\right) = \frac{-1+\sqrt{5}}{4}$ . The equation  $\cos(2\pi x) = \frac{-1+\sqrt{5}}{4}$  has two solutions  $x = \frac{1}{5}$  and  $x = \frac{4}{5}$ , for  $0 \leq x < 1$ . It follows that if  $n_2$  is a multiple of 5, we have that  $\frac{n_2}{5}, \frac{4n_2}{5} \in [0, n_2 - 1]$ . Since  $n_1$  and  $n_2$  can switch roles, in total, we get eight solutions for Eq. (7) if  $n_1 \bmod 5 \equiv 0$  and  $n_2 \bmod 5 \equiv 0$ . ◀

## 5 King's Graph and Strong Products

Again, let us start with some definitions. The *Strong product* of two graphs  $G_1$  and  $G_2$ , denoted by  $G_1 \boxtimes G_2$ , is the graph  $G = (V, E)$  where  $V = V_1 \times V_2$  and

$$E = \{(v, u), (v', u) : (v, v') \in E_1\} \cup \{(v, u), (v, u') : (u, u') \in E_2\} \cup \{(v, u), (v', u') : (v, v') \in E_1 \text{ and } (u, u') \in E_2\} .$$

The adjacency matrix of  $G_1 \boxtimes G_2$  is defined as  $A_{G_1 \boxtimes G_2} = \bar{A}_{G_1} \otimes \bar{A}_{G_2} - I_{|V_1||V_2|}$ .

► **Theorem 17** ([5]). *Let  $G_1$  and  $G_2$  be graphs. Then, the set of eigenvalues of  $A_{G_1 \boxtimes G_2}$  is*

$$\Lambda(A_{G_1 \boxtimes G_2}) = \{(\lambda + 1)(\mu + 1) - 1 \mid \lambda \in \Lambda(A_{G_1}), \mu \in \Lambda(A_{G_2})\} .$$

A king's graph is the Strong product of two paths (see Figure 1d). Underlying a king's graph has the topology of a grid graph. Here, the neighborhood of a vertex corresponds to a rectangular scanning window (see Figure 1c). Again, we use the product-property to determine the number of surgical probes directly, without using Theorem 2.

► **Theorem 18.** *Let  $G$  be a king's graph of dimensions  $n_1 \times n_2$ . The number of surgical probes that are sufficient to uncover  $\ell$  is  $\mathcal{I}_2^3(n_1)n_2 + \mathcal{I}_2^3(n_2)n_1 - \mathcal{I}_2^3(n_1)\mathcal{I}_2^3(n_2)$ .*

**Proof.** Due to Theorem 17 the number of required probes is given by the solutions of the equation:

$$\left(2 \cos\left(\frac{i}{n_1 + 1} \cdot \pi\right) + 1\right) \left(2 \cos\left(\frac{j}{n_2 + 1} \cdot \pi\right) + 1\right) = 0 , \quad (8)$$

for  $i = [1, n_1]$  and  $j = [1, n_2]$ . Equation (8) has solutions if one of the factors becomes zero. From the proof of Theorem 12, we know that the equation  $2 \cos\left(\frac{i\pi}{n_1 + 1}\right) = -1$  has one solution if  $n_1 \bmod 3 \equiv 2$ . In this case, we get a solution of Eq. (8) for each value of  $j$  if  $n_2 \bmod 3 \not\equiv 2$ . By symmetry we get  $n_1$  solutions if  $n_2 \bmod 3 \equiv 2$  and  $n_1 \bmod 3 \not\equiv 2$ . If  $n_1, n_2 \bmod 3 \equiv 2$ , we get  $n_1 + n_2 - 1$  solutions for Eq. (8). ◀

We see that king's graphs behave quite differently compared to grid graphs. Here, the number of required surgical probes can be as large as  $n_1 + n_2 - 1$ .

## 6 Future directions

We extended the MIR framework by representing the inspected object by an undirected graph. A probe corresponds to a measurement taken over the node and its neighborhood. There are many other potentially interesting types of probes in this general model of graphs. For example, when the specimen is a grid and a probe at a node contains all nodes at distance

at most  $d$  from this node. We gave a closed form formula for the number of surgical probes for the case where  $d = 1$  (grid graph and king's graph). It would be interesting to obtain such a formula for general  $d$ .

In the setting introduced here, the surgical probes have the same costs at each node. However, parts of a specimen might be less accessible and therefore more expensive to probe. It might be interesting to study a variation where a surgical probe at node  $i$  implies costs  $c_i$ , and the goal is now to uncover the labels with minimum total costs.

Moreover, considering directed graphs instead of un-directed graphs leads to a type of probes that are not symmetric. However, this implies that the adjacency matrix is no longer symmetric and Lemma 1 does not longer hold (see example on page 3 of [5]).

Another possible direction is to determine the minimum number of surgical probes in case  $\ell$  is a binary or integer vector. As mentioned earlier, our results provide an upper bound on the number of required surgical probes. This problem is most likely NP-hard as the work by Gritzmann et al. [9] suggests.

Finally, we conjecture that Theorem 6 can be extended to full  $k$ -ary trees.

---

## References

- 1 Andreas Alpers and Peter Gritzmann. Reconstructing binary matrices under window constraints from their row and column sums. *Fundamenta Informaticae*, 155(4):321–340, 2017.
- 2 Andreas Alpers and Peter Gritzmann. Dynamic discrete tomography. *Inverse Problems*, 34(3):034003, 2018.
- 3 Andreas Alpers and Peter Gritzmann. On double-resolution imaging and discrete tomography. *SIAM Journal on Discrete Mathematics*, 32(2):1369–1399, 2018.
- 4 Daniela Battaglino, Andrea Frosini, and Simone Rinaldi. A decomposition theorem for homogeneous sets with respect to diamond probes. *Computer Vision and Image Understanding*, 117(4):319–325, 2013.
- 5 Andries E. Brouwer and Willem H. Haemers. *Spectra of Graphs*. Springer, 2011.
- 6 John Conway and Alice J. Jones. Trigonometric diophantine equations (On vanishing sums of roots of unity). *Acta Arithmetica*, 30(3):229–240, 1976.
- 7 Andrea Frosini and Maurice Nivat. Binary matrices under the microscope: A tomographical problem. *Theor. Comput. Sci.*, 370(1-3):201–217, 2007.
- 8 Andrea Frosini, Maurice Nivat, and Simone Rinaldi. Scanning integer matrices by means of two rectangular windows. *Theoretical Computer Science*, 406(1-2):90–96, 2008.
- 9 Peter Gritzmann, Barbara Langfeld, and Markus Wiegmann. Uniqueness in discrete tomography: three remarks and a corollary. *SIAM Journal on Discrete Mathematics*, 25(4):1589–1599, 2011.
- 10 Gabor T Herman and Attila Kuba. *Discrete tomography: Foundations, algorithms, and applications*. Springer Science & Business Media, 2012.
- 11 Carl D Meyer. *Matrix analysis and applied linear algebra*, volume 71. Siam, 2000.
- 12 Maurice Nivat. Sous-ensembles homogènes de  $\mathbb{Z}^2$  et pavages du plan. *Comptes Rendus Mathématique*, 335(1):83–86, 2002.
- 13 Ivan Niven. *Numbers: rational and irrational*, volume 1. Random House New York, 1961.